

1 **Coarse particulate matter air quality in East Asia:**  
2 **implications for fine particulate nitrate**

3 Shixian Zhai<sup>1,\*</sup>, Daniel J. Jacob<sup>1</sup>, Drew C. Pendergrass<sup>1</sup>, Nadia K. Colombi<sup>2</sup>, Viral Shah<sup>1</sup>,  
4 Laura Hyesung Yang<sup>1</sup>, Qiang Zhang<sup>3</sup>, Shuxiao Wang<sup>4</sup>, Hwajin Kim<sup>5</sup>, Yele Sun<sup>6</sup>, Jin-Soo  
5 Choi<sup>7</sup>, Jin-Soo Park<sup>7</sup>, Gan Luo<sup>8</sup>, Fangqun Yu<sup>8</sup>, Jung-Hun Woo<sup>9</sup>, Younha Kim<sup>10</sup>, Jack E.  
6 Dibb<sup>11</sup>, Taehyoung Lee<sup>12</sup>, Jin-Seok Han<sup>13</sup>, Bruce E. Anderson<sup>14</sup>, Ke Li<sup>15</sup>, Hong Liao<sup>15</sup>

7  
8 <sup>1</sup> John A. Paulson School of Engineering and Applied Sciences, Harvard University, Cambridge, MA 02138

9 <sup>2</sup> Department of Earth and Planetary Science, Harvard University, Cambridge, MA 02138, USA

10 <sup>3</sup> Department of Earth System Science, Tsinghua University, Beijing 100084, China

11 <sup>4</sup> State Key Joint Laboratory of Environmental Simulation and Pollution Control, School of Environment,  
12 Tsinghua University, Beijing 100084, China

13 <sup>5</sup> Department of Environmental Health Sciences, Graduate School of Public Health, Seoul National  
14 University, Seoul 08826, South Korea

15 <sup>6</sup> State Key Laboratory of Atmospheric Boundary Layer Physics and Atmospheric Chemistry, Institute of  
16 Atmospheric Physics, Chinese Academy of Sciences, Beijing 100029, China

17 <sup>7</sup> Air Quality Research Division, National Institute of Environmental Research, Incheon 22689, Republic of  
18 Korea

19 <sup>8</sup> Atmospheric Sciences Research Center, University at Albany, Albany, NY 12226, USA

20 <sup>9</sup> Department of Civil and Environmental Engineering, Konkuk University, Seoul 05029, South Korea

21 <sup>10</sup> International Institute for Applied Systems Analysis (IIASA), Laxenburg 2361, Austria

22 <sup>11</sup> Institute for the Study of Earth, Oceans, and Space, University of New Hampshire, Durham, NH 03824

23 <sup>12</sup> Department of Environmental Science, Hankuk University of Foreign Studies, Yongin 449791, South  
24 Korea

25 <sup>13</sup> Department of Environmental and Energy Engineering, Anyang University, Anyang 14028, South Korea

26 <sup>14</sup> NASA Langley Research Center, Hampton, VA 23681, USA

27 <sup>15</sup> Jiangsu Key Laboratory of Atmospheric Environment Monitoring and Pollution Control, Collaborative  
28 Innovation Center of Atmospheric Environment and Equipment Technology, School of Environmental  
29 Science and Engineering, Nanjing University of Information Science and Technology, Nanjing 210044,  
30 China

31 *Correspondence to:* Shixian Zhai (zhaisx@g.harvard.edu)

32

33 **Abstract.** Air quality network data in China and South Korea show very high year-round mass  
34 concentrations of coarse particulate matter (PM), as inferred by difference between  $PM_{10}$  and  $PM_{2.5}$ . Coarse  
35 PM concentrations in 2015 averaged  $52 \mu\text{g m}^{-3}$  in the North China Plain (NCP) and  $23 \mu\text{g m}^{-3}$  in the Seoul  
36 Metropolitan Area (SMA), contributing nearly half of  $PM_{10}$ . Strong daily correlations between coarse PM  
37 and carbon monoxide imply a dominant source from anthropogenic fugitive dust. Coarse PM  
38 concentrations in the NCP and the SMA decreased by 21% from 2015 to 2019 and further dropped abruptly  
39 in 2020 due to COVID-19 reductions in construction and vehicle traffic. Anthropogenic coarse PM is  
40 generally not included in air quality models but scavenges nitric acid to suppress the formation of fine  
41 particulate nitrate, a major contributor to  $PM_{2.5}$  pollution. GEOS-Chem model simulation of surface and  
42 aircraft observations from the KORUS-AQ campaign over the SMA in May-June 2016 shows that  
43 consideration of anthropogenic coarse PM largely resolves the previous model overestimate of fine  
44 particulate nitrate. The effect is smaller in the NCP which has a larger excess of ammonia. Model  
45 sensitivity simulations for 2015-2019 show that decreasing anthropogenic coarse PM directly increases  
46  $PM_{2.5}$  nitrate in summer, offsetting 80% the effect of nitrogen oxide and ammonia emission controls, while  
47 in winter the presence of coarse PM increases the sensitivity of  $PM_{2.5}$  nitrate to ammonia and sulfur dioxide  
48 emissions. Decreasing coarse PM helps to explain the lack of decrease in wintertime  $PM_{2.5}$  nitrate observed  
49 in the NCP and the SMA over the 2015-2021 period despite decreases in nitrogen oxide and ammonia  
50 emissions. Continuing decrease of fugitive dust pollution means that more stringent nitrogen oxide and  
51 ammonia emission controls will be required to successfully decrease  $PM_{2.5}$  nitrate.

## 52 1. Introduction

53 Coarse particulate matter (coarse PM; particulate matter between  $2.5 \mu\text{m}$  and  $10 \mu\text{m}$  aerodynamic diameter)  
54 is a severe air pollution problem in East Asia, contributing a particle mass comparable to fine particulate  
55 matter ( $PM_{2.5}$ ) and thus about half of  $PM_{10}$  (Chen et al., 2019; Lee et al., 2015; Qiu et al., 2014; Wang et al.,  
56 2018a). It is mainly fugitive mineral dust, with contributions from both natural desert dust and  
57 anthropogenic sources including on-road traffic, construction, and agriculture (Wu et al., 2016; Zhao et al.,  
58 2017; Liu et al., 2021; Kutra, 2020). Atmospheric chemistry models used in air quality applications  
59 generally do not include anthropogenic fugitive dust, due to the lack of available emission inventories  
60 except for a few urban areas (Li et al., 2021a; Li et al., 2021b; Li et al., 2021c). Aside from its direct  
61 interest as an air pollutant, coarse PM can suppress  $PM_{2.5}$  by heterogeneously taking up acids ( $\text{HNO}_3$ ,  $\text{SO}_2$ ,  
62 and  $\text{H}_2\text{SO}_4$ ) that would otherwise lead to  $PM_{2.5}$  formation. This uptake has been observed for natural dust  
63 events (Wang et al., 2017; Heim et al., 2020; Wang et al., 2018b; Park et al., 2004; Stone et al., 2011), but  
64 the more ubiquitous effect from anthropogenic dust has received little study (Kakavas and Pandis, 2021;  
65 Hodzic et al., 2006). With increasingly stringent control measures to decrease fugitive dust air pollution in  
66 East Asia (Chinese State Council, 2019; Noh et al., 2018; Wu et al., 2016; Xing et al., 2018), it is important  
67 to better understand the impact on  $PM_{2.5}$  air quality.

68 A specific issue is the effect of anthropogenic dust on PM<sub>2.5</sub> nitrate. Nitrate is a major component of  
69 PM<sub>2.5</sub> in urban regions of East Asia including the North China Plain (NCP) (Li et al., 2019; Zhai et al.,  
70 2021a) and the Seoul Metropolitan Area (SMA) (Jeong et al., 2022; Kim et al., 2020), and it can dominate  
71 haze pollution events in both regions (Fu et al., 2020; Li et al., 2018; Xu et al., 2019; Kim et al., 2017; Kim  
72 et al., 2020). PM<sub>2.5</sub> nitrate over North China in winter has not decreased in recent years despite reductions  
73 in emissions of the precursor nitrogen oxides (NO<sub>x</sub> ≡ NO + NO<sub>2</sub>) (Zhai et al., 2021a; Fu et al., 2020) from  
74 fossil fuel combustion. This has been attributed to limitation by ammonia (NH<sub>3</sub>) emissions, since PM<sub>2.5</sub>  
75 nitrate is mainly present as ammonium nitrate (Zhai et al., 2021a). Decreasing coarse PM emissions is  
76 another possible explanation as it would allow more HNO<sub>3</sub> to be available for PM<sub>2.5</sub> nitrate formation, and  
77 it could also shift PM<sub>2.5</sub> nitrate formation to be more NH<sub>3</sub>-limited. Better understanding this sensitivity of  
78 PM<sub>2.5</sub> nitrate to coarse PM is of crucial importance because of recent efforts by the Chinese government to  
79 decrease NH<sub>3</sub> emissions (Liao et al., 2022), which are mainly from agriculture with additional urban  
80 contributions from vehicle, industrial, and waste disposal sources (Mgelwa et al., 2022).

81 In this work, we show that coarse PM over the NCP and the SMA is mainly anthropogenic and decreased  
82 by 21% during the 2015-2019 period. We find that accounting for this anthropogenic coarse PM in the  
83 GEOS-Chem atmospheric chemistry model greatly improves the ability of the model to simulate PM<sub>2.5</sub>  
84 nitrate during the KORUS-AQ aircraft campaign over Korea where previous GEOS-Chem simulations  
85 found a large overestimate (Travis et al., 2022; Zhai et al., 2021b). From there we examine the implications  
86 for the effects of emission controls on long-term trends of PM<sub>2.5</sub> nitrate in China and South Korea.

## 87 2. Coarse PM in China and South Korea

88 Figure 1 shows the annual mean concentrations of coarse PM in 2015, 2019, and 2020 measured at air  
89 quality networks in China and South Korea as the PM<sub>10</sub> – PM<sub>2.5</sub> difference. Data for China are from the  
90 Ministry of Ecology and Environment (MEE) network (<http://www.quotsoft.net/air/>) and data for South  
91 Korea are from the AirKorea network (<https://www.airkorea.or.kr>). We remove spurious data when PM<sub>2.5</sub> is  
92 higher than PM<sub>10</sub>, which account for 1.7% and 0.2% of the dataset respectively in China and South Korea.

93 We see from Fig. 1 that coarse PM concentrations in China and South Korea are highest in the NCP and  
94 the SMA, respectively, indicating a dominant urban anthropogenic origin. Coarse PM in year 2015  
95 averaged 52 μg m<sup>-3</sup> in the NCP and 23 μg m<sup>-3</sup> in the SMA, contributing nearly half of total PM<sub>10</sub> (120 μg m<sup>-3</sup>  
96 in the NCP and 50 μg m<sup>-3</sup> in the SMA). National air quality standards for annual mean PM<sub>10</sub> are 70 μg m<sup>-3</sup>  
97 in China (urban) and 50 μg m<sup>-3</sup> in South Korea, well above the World Health Organization (WHO)  
98 recommended annual standard of 15 μg m<sup>-3</sup>. Coarse PM decreased by 21% in both the NCP and the SMA  
99 from 2015 to 2019, reflecting emission controls on fugitive dust (Chinese State Council, 2013, 2018; Noh  
100 et al., 2018; Wu et al., 2016), and further decreased strongly in 2020 because of COVID-19 restrictions on

101 traffic and construction. The COVID-19 impact is evident in China by comparing concentrations before  
102 and after the sharp January 24, 2020 lockdown (Fig. 2).

103 Figure 3 shows further evidence of the dominant anthropogenic contribution to coarse PM as the daily  
104 correlation with carbon monoxide (CO) in 2015. CO is emitted by incomplete combustion and is a tracer of  
105 urban influence. We find strong correlations between coarse PM and CO with consistent slopes except in  
106 spring, which features high coarse PM outliers attributable to desert dust events (Heim et al., 2020; Shao  
107 and Dong, 2006). Similar correlations to 2015 are found in other years (Fig. S1). The desert dust events  
108 drive the seasonal maximum of coarse PM in Fig. 1h.

### 109 **3. Effect of anthropogenic coarse PM on fine particulate nitrate during KORUS-AQ**

110 We simulated the effect of anthropogenic coarse PM on PM<sub>2.5</sub> nitrate using the GEOS-Chem model and  
111 evaluated the model with observations from the KORUS-AQ aircraft campaign over South Korea in May-  
112 June 2016 (Crawford et al., 2021). KORUS-AQ offers a unique data set of detailed aerosol and gas-phase  
113 composition over East Asia. Previous GEOS-Chem simulations showed a large overestimate of fine  
114 particulate nitrate and a large underestimate of coarse PM (Travis et al., 2022; Zhai et al., 2021b).  
115 Particulate nitrate concentrations were measured during KORUS-AQ at the Korea Institute of Science and  
116 Technology (KIST) surface site and on the aircraft by Aerosol Mass Spectrometers (AMS) with size cut of  
117 1  $\mu\text{m}$  diameter (PM<sub>1</sub> nitrate) (Kim et al., 2017; Kim et al., 2018). The AMS only detects non-refractory  
118 nitrate, taken here to be ammonium nitrate (Fig. S2). Total particulate nitrate with size cut of 4  $\mu\text{m}$  diameter  
119 (PM<sub>4</sub> nitrate) was also sampled on the aircraft by the Soluble Acidic Gases and Aerosol (SAGA) instrument  
120 (Dibb et al., 2003; McNaughton et al., 2007). Additional measurements on the aircraft included HNO<sub>3</sub>  
121 concentrations with a Chemical Ionization Time of Flight Mass Spectrometer (CIT-ToF-CIMS), and  
122 aerosol size distributions including coarse PM with a DMT CPSPD Probe. We focus on the observations  
123 over the SMA and exclude observations from two process-directed flights (RF7 and RF8) and the Daesan  
124 power plant plume following Park et al. (2021).

125 We use GEOS-Chem version 13.0.2 (<https://zenodo.org/record/4681204>) in a nested-grid simulation  
126 over East Asia (100 - 150° E, 20 - 50° N) with a horizontal resolution of 0.5° $\times$ 0.625°. The model simulates  
127 detailed oxidant-aerosol chemistry relevant to PM<sub>2.5</sub> nitrate formation (Zhai et al., 2021a) and is driven by  
128 meteorological data from the NASA Modern-Era Retrospective Analysis for Research and Applications,  
129 Version 2 (MERRA-2). Formation of semi-volatile ammonium nitrate aerosol is governed by ISORROPIA  
130 version 2.2 thermodynamics (Fountoukis and Nenes, 2007). Dry deposition of gases and particles follows a  
131 standard resistance-in-series scheme (Wesely, 1989). Wet deposition of gases and particles includes  
132 contributions from rainout, washout, and scavenging in convective updrafts (Liu et al., 2001; Luo et al.,  
133 2019). The model includes reactive uptake of HNO<sub>3</sub> on dust limited by dust alkalinity and mass transfer  
134 (Fairlie et al., 2010), assuming 7.1 % Ca<sup>2+</sup> and 1.1% Mg<sup>2+</sup> as carbonates per mass in emitted dust (Shah et

135 al., 2020a; Tang and Han, 2017; Zhang et al., 2014). The relative humidity (RH)-dependent reactive uptake  
136 coefficient ( $\gamma$ ) of  $\text{HNO}_3$  is based on laboratory studies (Liu et al., 2008; Huynh and McNeill, 2020) and  
137 observations during natural dust events in Beijing (Tian et al., 2021; Wang et al., 2017), and increases from  
138 0.06 to 0.21 as RH increases from 40% to 80%. Monthly anthropogenic emissions for China are from the  
139 Multi-resolution Emission Inventory for China (MEIC) (Zheng et al., 2018; Zheng et al., 2021a; Zheng et  
140 al., 2021b), and emissions for other Asian countries including South Korea are from the KORUSv5  
141 inventory (Woo et al., 2020). Fine anthropogenic mineral dust emissions from combustion and industrial  
142 sources (ash) are derived from the MEIC and KORUSv5 inventories as the residual of anthropogenic  
143 primary  $\text{PM}_{2.5}$  emissions after excluding primary organic aerosol, black carbon, and primary sulfate (Philip  
144 et al., 2017).

145 We compare the results from the standard model as described above to a simulation where we add  
146 anthropogenic coarse PM by using 24-hour average observed coarse PM concentrations from the air quality  
147 networks (Fig. 1) as boundary conditions at the lowest model level. For this purpose, we linearly interpolate  
148 the daily mean coarse PM data from the network to the GEOS-Chem model horizontal grid and apply them  
149 to the coarse dust GEOS-Chem model component with an effective diameter of 4.8  $\mu\text{m}$ . This concentration  
150 boundary condition in the lowest model level serves as an implicit source and defines the vertical  
151 concentration profile. The resulting vertical profiles of coarse PM in GEOS-Chem over South Korea are  
152 consistent with KORUS-AQ aircraft observations (Fig. S3). Anthropogenic coarse PM is assumed to be  
153 mainly fugitive dust with the same alkalinity properties as natural dust (Zhang et al., 2014; Tang and Han,  
154 2017).

155 Figure 4 compares GEOS-Chem to the KORUS-AQ observations including median diurnal  $\text{PM}_1$  nitrate  
156 at the KIST site and median aircraft vertical profiles over the SMA. The model is sampled along the aircraft  
157 flight tracks at the times of the observations, all in daytime.  $\text{PM}_{1-4}$  nitrate is derived as the difference  
158 between SAGA  $\text{PM}_4$  nitrate and AMS  $\text{PM}_1$  nitrate. Here we take ammonium nitrate in the model for  
159 comparison to  $\text{PM}_1$  observations, and size-resolved dust nitrate for comparison to  $\text{PM}_{1-4}$  observations. In  
160 this way, any dust-associated refractory  $\text{PM}_1$  nitrate is included in the  $\text{PM}_{1-4}$  profiles, for both observations  
161 and the GEOS-Chem model. Such classification does not allow for supermicron ammonium nitrate, but  
162 KORUS-AQ observations found ammonium nitrate to be mainly submicron (Kim et al., 2018). GEOS-  
163 Chem results are shown both for the standard model (not including anthropogenic coarse PM) and with the  
164 addition of anthropogenic coarse PM. In both simulations, we adjusted the diurnal variation of  $\text{NH}_3$   
165 emission to match the  $\text{NH}_3$  observations made at the Olympic Park site, 7 km southeast of KIST (Fig. S4).

166 The standard GEOS-Chem simulation without anthropogenic fugitive dust overestimates daytime  $\text{PM}_1$   
167 nitrate (aircraft and surface) by about a factor of two while underestimating  $\text{PM}_{1-4}$  nitrate by about a factor  
168 of two (Fig. 4a, b, and c). Coarse PM in the standard simulation (from natural dust and sea salt) is near

169 zero, in contrast to observations (Fig. 4d). Adding anthropogenic coarse PM to the model corrects this bias  
170 and further corrects the  $PM_1$  and  $PM_{1-4}$  nitrate biases by providing an added sink for  $HNO_3$ . We find that  
171 anthropogenic coarse PM takes up  $HNO_3$  three times faster than dry deposition and that this uptake is  
172 limited by mass-transfer rather than alkalinity (only 60-70% of the coarse dust alkalinity in surface air is  
173 neutralized on average). The shift from  $PM_1$  to  $PM_{1-4}$  nitrate is consistent with the uptake of  $HNO_3$  by  
174 coarse PM, with some of this uptake in the model taking place on dust coarser than  $4\ \mu m$  and so not  
175 observed by  $PM_{1-4}$  nitrate. Half of the model overestimate of  $HNO_3$  is corrected (Fig. 4e), with the  
176 remainder possibly due to an underestimate of  $HNO_3$  deposition velocity (Travis et al., 2022). The model  
177 overestimates nighttime nitrate in surface air at the KIST site, even with anthropogenic coarse PM. This  
178 nighttime nitrate in the model is driven by heterogeneous  $NO_2$  and  $N_2O_5$  chemistry under stratified  
179 conditions, which could be subject to large local errors (Travis et al., 2022).

180 We also examined the effect of anthropogenic coarse PM on  $PM_{2.5}$  nitrate concentrations in the NCP.  
181  $PM_{2.5}$  nitrate observations in NCP are mostly filter-collected bulk  $PM_{2.5}$  nitrate, which could be biased low  
182 in summer due to volatilization (Chow et al., 2005). Previous evaluation of GEOS-Chem with 2013 and  
183 2015  $PM_{2.5}$  nitrate observations across China in summer and winter found no significant bias in 2015 or  
184 winter 2013 but an overestimate in summer 2013 (Zhai et al., 2021a). That simulation did not include  
185  $HNO_3$  uptake by dust (natural or anthropogenic). We find here that including  $HNO_3$  uptake by fine ( $PM_{2.5}$ )  
186 dust has little effect on total  $PM_{2.5}$  nitrate but partitions 10% of ammonium nitrate mass to fine dust nitrate  
187 in winter and 23% in summer (Fig. S5). Adding anthropogenic coarse PM in GEOS-Chem decreases  
188 modeled ammonium nitrate in the NCP by 10-20% in winter and by 25-30% in summer, a relatively more  
189 modest effect than over the SMA because of larger excess of  $NH_3$ . The comparison with  $PM_{2.5}$  nitrate  
190 observations here indicates that fine dust associated nitrate should be considered when comparing modeled  
191 particle nitrate to bulk  $PM_{2.5}$  nitrate data.

#### 192 **4. Implications for long-term trends of $PM_{2.5}$ nitrate and responses to emission controls**

193 There are to our knowledge no readily accessible continuous long-term records of  $PM_{2.5}$  nitrate  
194 concentrations in China or South Korea. Figure 5 shows a multi-year compilation of winter and summer  
195 mean  $PM_1$  and  $PM_{2.5}$  nitrate observations from individual field campaigns in Beijing and Seoul over 2015-  
196 2021 (Table S1). We find no significant trends in winter, consistent with previous studies in the NCP that  
197 examined earlier periods (Fu et al., 2020). In summer, observations tend to show a decrease over the period  
198 but with large interannual variations driven by meteorology (Li et al., 2018; Zhai et al., 2021a).

199 Changes in anthropogenic emissions of  $NO_x$ ,  $SO_2$ ,  $NH_3$ ,  $PM_{2.5}$ , and coarse PM could all affect  $PM_{2.5}$   
200 nitrate, and we used GEOS-Chem to investigate these effects for the 2015-2019 period. The Multi-  
201 resolution Emission Inventory for China (MEIC) reports that  $NO_x$  emissions in the NCP decreased by 11%  
202 from 2015 to 2019,  $SO_2$  emissions decreased by 54%, and primary  $PM_{2.5}$  from combustion decreased by

203 35% (Zheng et al., 2021a). This primary PM<sub>2.5</sub> includes a 40% contribution from mineral ash that we treat  
204 as anthropogenic fine dust and decreased by 27% from 2015 to 2019. The MEIC also reports a 15%  
205 decrease of NH<sub>3</sub> emissions over China from 2015 to 2019 (19% for the NCP), while the PKU-NH<sub>3</sub>  
206 emission inventory reports a 6% decrease over China from 2015 to 2018 (Liao et al., 2022). Observations  
207 of surface NO<sub>2</sub> and SO<sub>2</sub> over the SMA imply a 22% decrease of NO<sub>x</sub> emissions and a 40% decrease of SO<sub>2</sub>  
208 emissions from 2015 to 2019 (Bae et al., 2021; Colombi et al., 2022). Coarse PM decreased by 33% over  
209 the NCP and by 31% over SMA during the same period (considering winter and summer data only).

210 Figure 6 shows the resulting emission-driven changes of PM<sub>2.5</sub> nitrate over the NCP and SMA from 2015  
211 to 2019 as simulated by GEOS-Chem in sensitivity simulations applying either 2015 or 2019 emissions to  
212 the same meteorological year (2019), and with or without anthropogenic coarse PM. The sum of changes  
213 driven by individual emission changes amounts to the total emission-driven net change. Sensitivities to  
214 NH<sub>3</sub> and primary PM<sub>2.5</sub> emissions in the SMA are solely driven by emission trends in China since we  
215 assume no emission trends for these species in South Korea.

216 The model reproduces the lack of trend in winter and the decreasing trend in summer seen in the  
217 observations for both the NCP and SMA. The lack of trend in winter reflects offsetting influences from  
218 decreasing NO<sub>x</sub>, NH<sub>3</sub>, and primary PM<sub>2.5</sub> emissions on the one hand, and decreasing SO<sub>2</sub> and coarse PM  
219 emissions on the other hand. Decreasing SO<sub>2</sub> increases the availability of NH<sub>3</sub> for nitrate formation (Fu et  
220 al., 2020; Zhai et al., 2021a). Decreasing primary PM<sub>2.5</sub> reduces the aerosol volume available for  
221 heterogeneous conversion of NO<sub>x</sub> to HNO<sub>3</sub> (Shah et al., 2020b). Decreasing coarse PM has relatively little  
222 direct effect on PM<sub>2.5</sub> nitrate in winter in the NCP because abundant atmospheric NH<sub>3</sub> combined with low  
223 temperatures drives HNO<sub>3</sub> near-quantitatively to ammonium-nitrate particles, and subsequent mass transfer  
224 of HNO<sub>3</sub> from ammonium nitrate to coarse PM is very slow because of the weak HNO<sub>3</sub> partial pressure  
225 (Wexler and Seinfeld, 1992). The decrease of coarse PM still quantitatively offsets the benefit from NO<sub>x</sub>  
226 emission controls, which has been the main vehicle for controlling PM<sub>2.5</sub> nitrate. Consideration of coarse  
227 PM in the model further increases the sensitivity of PM<sub>2.5</sub> nitrate to NH<sub>3</sub> and SO<sub>2</sub> emissions respectively by  
228 30% and 46%. This is because coarse PM provides an additional sink for the small fraction of HNO<sub>3</sub> that  
229 remains in the gas phase, which increases the sensitivity of the atmospheric lifetime of total nitrate  
230 (ammonium nitrate + HNO<sub>3</sub>) to changes in NH<sub>3</sub> or SO<sub>2</sub> emissions (Zhai et al., 2021a).

231 In summer, we find that the decrease in coarse PM over the 2015-2019 period directly cancels half of the  
232 benefit from decreasing NO<sub>x</sub>, SO<sub>2</sub>, NH<sub>3</sub>, and primary PM<sub>2.5</sub> emissions in the NCP, with less effect in the  
233 SMA. Over the NCP, the decrease of coarse PM offsets 80% of the benefits from NO<sub>x</sub> and NH<sub>3</sub> emission  
234 controls. Unlike in winter, decreasing SO<sub>2</sub> suppresses nitrate formation by decreasing the aerosol liquid  
235 water content (Stelson and Seinfeld, 1982). The effect of decreasing coarse PM emissions in summer is  
236 larger than in winter because warmer temperatures allow more HNO<sub>3</sub> to remain in the gas phase under

237  $\text{NH}_3\text{-HNO}_3\text{-H}_2\text{SO}_4$  thermodynamics and thus be scavenged by coarse PM.

## 238 **5. Conclusions**

239 Coarse PM ( $\text{PM}_{10}$  -  $\text{PM}_{2.5}$ ) in urban areas of China and South Korea is very high year-round and is mainly  
240 of anthropogenic origin as fugitive dust except for natural desert dust events in spring. Annual mean coarse  
241 PM concentrations decreased by 21% from 2015 to 2019 in both the North China Plain (NCP) and the  
242 Seoul Metropolitan Area (SMA), with steeper decreases in 2020 because of COVID-19 restrictions on  
243 traffic and construction. Considering only winter and summer when the influence of natural dust is small,  
244 we find that anthropogenic fugitive dust emissions decreased by about 30% from 2015 to 2019 in both the  
245 NCP and the SMA.

246 Anthropogenic coarse PM is of direct air quality concern because it accounts for about half of total  $\text{PM}_{10}$   
247 in the NCP and the SMA, but it also takes up  $\text{HNO}_3$  effectively and can thus suppress formation of fine  
248 particulate nitrate which is a major component of  $\text{PM}_{2.5}$  pollution. Comparison of GEOS-Chem model  
249 simulations to surface and aircraft observations from the KORUS-AQ campaign over the SMA in May-  
250 June 2016 shows that accounting for anthropogenic coarse PM largely corrects previous model  
251 overestimates of fine particulate nitrate.

252 Decrease in anthropogenic coarse PM emissions to improve  $\text{PM}_{10}$  air quality could have the unintended  
253 consequence of increasing  $\text{PM}_{2.5}$  nitrate, offsetting the gains from decreases in  $\text{NO}_x$  and  $\text{NH}_3$  emissions.  
254 Compilation of 2015-2021 observations of fine particulate nitrate in Beijing and Seoul suggests little trend  
255 in winter and a decrease in summer, consistent with GEOS-Chem. Decreasing coarse PM in the model in  
256 winter offsets the benefit of decreasing  $\text{NO}_x$  emissions, and coarse PM further increases the sensitivity of  
257  $\text{PM}_{2.5}$  nitrate to changes in  $\text{NH}_3$  and  $\text{SO}_2$  emissions by affecting the lifetime of total inorganic nitrate  
258 (ammonium nitrate +  $\text{HNO}_3$ ). In summer, decreasing coarse PM in the NCP offsets 80% of the  $\text{PM}_{2.5}$  nitrate  
259 benefit of decreasing  $\text{NO}_x$  and  $\text{NH}_3$  emissions. As coarse PM continues to decrease in response to fugitive  
260 dust pollution control, there is a greater need to reduce  $\text{NH}_3$  and  $\text{NO}_x$  emissions in order to decrease fine  
261 particulate nitrate air pollution in East Asia.

262

263 *Data availability.*  $\text{PM}_{2.5}$ ,  $\text{PM}_{10}$ , and CO data over China are from <http://www.quotsoft.net/air/>, over South  
264 Korea are from [https://www.airkorea.or.kr/web/last\\_amb\\_hour\\_data?pMENU\\_NO=123](https://www.airkorea.or.kr/web/last_amb_hour_data?pMENU_NO=123). Surface and  
265 aircraft data during KORUS-AQ are from <https://doi.org/10.5067/Suborbital/KORUSAQ/DATA01>. Multi-  
266 year compilation of winter and summer mean  $\text{PM}_1$  and  $\text{PM}_{2.5}$  nitrate are provided in Table S1.

267

268 *Supplement.* The supplement related to this article is uploaded at submission.

269



270 *Author Contributions.* S.Z. and D.J.J. designed the research. S.Z. performed the research. D.C.P., N.K.C.,  
271 V.S., L.H.Y., and H.L. helped with data analysis and results interpretation. Q.Z. provided the MEIC  
272 emission inventory. S.W., H.K., Y.S., J.S.C, J.S.P., J.E.D., T.L., J.S.H, and B.E.A provided observation  
273 data. J.H.W. and Y.K. provided the KORUSv5 emission inventory. G.L., F.Y., and K.L. helped with model  
274 simulations. S.Z. and D.J.J wrote the paper with input from all other authors.

275

276 *Competing Interests.* The authors declare no competing interests.

277

278 *Financial support.* This work was funded by the Harvard–NUIST Joint Laboratory for Air Quality and  
279 Climate (JLAQC) and the Samsung Advanced Institute of Technology.

280

281 *Acknowledgments.* We thank Bo Zheng (Tsinghua Shenzhen International Graduate School, Tsinghua  
282 University) for processing the MEIC emission inventory. We thank Paul O. Wennberg, Michelle J. Kim,  
283 Alexander P. Teng, and John D. Crouse from the California Institute of Technology for their contributions  
284 to HNO<sub>3</sub> measurements during KORUS-AQ.

285

## 286 **References**

287 Bae, M., Kim, B.-U., Kim, H. C., Kim, J., and Kim, S.: Role of emissions and meteorology in the  
288 recent PM<sub>2.5</sub> changes in China and South Korea from 2015 to 2018, *Environ. Pollut.*, 270,  
289 116233, <https://doi.org/10.1016/j.envpol.2020.116233>, 2021.

290 Chen, R., Yin, P., Meng, X., Wang, L., Liu, C., Niu, Y., Liu, Y., Liu, J., Qi, J., You, J., Kan, H.,  
291 and Zhou, M.: Associations between Coarse Particulate Matter Air Pollution and Cause-  
292 Specific Mortality: A Nationwide Analysis in 272 Chinese Cities, *Environ. Health Perspect.*,  
293 127, 017008, <https://doi.org/10.1289/EHP2711>, 2019.

294 Chow, J. C., Watson, J. G., Lowenthal, D. H., and Magliano, K. L.: Loss of PM<sub>2.5</sub> nitrate from  
295 filter samples in central California, *J. Air Waste Manag. Assoc.*, 55, 1158-1168,  
296 <https://doi.org/10.1080/10473289.2005.10464704>, 2005.

297 Colombi, N. K., Jacob, D. J., Yang, L. H., Zhai, S., Shah, V., Grange, S. K., Yantosca, R. M.,  
298 Kim, S., and Liao, H.: Why is ozone in South Korea and the Seoul Metropolitan Area so  
299 high and increasing?, *EGUsphere*, 2022, 1-21, 10.5194/egusphere-2022-1366, 2022.

300 Chinese State Council: Action Plan on Prevention and Control of Air Pollution,  
301 [http://www.gov.cn/zwggk/2013-09/12/content\\_2486773.htm](http://www.gov.cn/zwggk/2013-09/12/content_2486773.htm) (last access: December 18  
302 2022), 2013 (in Chinese).

303 Chinese State Council: Three-year Action Plan for Protecting Blue Sky,  
304 [http://www.gov.cn/zhengce/content/2018-07/03/content\\_5303158.htm](http://www.gov.cn/zhengce/content/2018-07/03/content_5303158.htm) (last access:  
305 December 18 2022), 2018 (in Chinese).

306 Chinese State Council: Beijing has set up more than 1,000 sites to monitor dust,  
307 [http://www.gov.cn/xinwen/2019-04/16/content\\_5383488.htm](http://www.gov.cn/xinwen/2019-04/16/content_5383488.htm) (last access: December 18  
308 2022), 2019 (in Chinese).

309 Crawford, J. H., Ahn, J.-Y., Al-Saadi, J., Chang, L., Emmons, L. K., Kim, J., Lee, G., Park, J.-H.,  
310 Park, R. J., Woo, J. H., Song, C.-K., Hong, J.-H., Hong, Y.-D., Lefer, B. L., Lee, M., Lee,  
311 T., Kim, S., Min, K.-E., Yum, S. S., Shin, H. J., Kim, Y.-W., Choi, J.-S., Park, J.-S.,  
312 Szykman, J. J., Long, R. W., Jordan, C. E., Simpson, I. J., Fried, A., Dibb, J. E., Cho, S., and  
313 Kim, Y. P.: The Korea–United States Air Quality (KORUS-AQ) field study, *Elementa-Sci.*  
314 *Anthrop.*, 9 (1), 1-27, <https://doi.org/10.1525/elementa.2020.00163>, 2021.

315 Dibb, J. E., Talbot, R. W., Scheuer, E. M., Seid, G., Avery, M. A., and Singh, H. B.: Aerosol  
316 chemical composition in Asian continental outflow during the TRACE-P campaign:  
317 Comparison with PEM-West B, *J. Geophys. Res. Atmos.*, 108, 8815,  
318 <https://doi.org/10.1029/2002JD003111>, 2003.

319 Fairlie, T. D., Jacob, D. J., Dibb, J. E., Alexander, B., Avery, M. A., van Donkelaar, A., and  
320 Zhang, L.: Impact of mineral dust on nitrate, sulfate, and ozone in transpacific Asian  
321 pollution plumes, *Atmos. Chem. Phys.*, 10, 3999-4012, [https://doi.org/10.5194/acp-10-3999-](https://doi.org/10.5194/acp-10-3999-2010)  
322 [2010](https://doi.org/10.5194/acp-10-3999-2010), 2010.

323 Fountoukis, C. and Nenes, A.: ISORROPIA II: a computationally efficient thermodynamic  
324 equilibrium model for  $K^+$ - $Ca^{2+}$ - $Mg^{2+}$ - $NH_4^+$ - $Na^+$ - $SO_4^{2-}$ - $NO_3^-$ - $Cl^-$ - $H_2O$  aerosols, *Atmos.*  
325 *Chem. Phys.*, 7, 4639-4659, <https://doi.org/10.5194/acp-7-4639-2007>, 2007.

326 Fu, X., Wang, T., Gao, J., Wang, P., Liu, Y., Wang, S., Zhao, B., and Xue, L.: Persistent Heavy  
327 Winter Nitrate Pollution Driven by Increased Photochemical Oxidants in Northern China,  
328 *Environ. Sci. Technol.*, 54, 3881–3889, <https://doi.org/10.1021/acs.est.9b07248>, 2020.

329 Heim, E. W., Dibb, J., Scheuer, E., Jost, P. C., Nault, B. A., Jimenez, J. L., Peterson, D., Knote,  
330 C., Fenn, M., Hair, J., Beyersdorf, A. J., Corr, C., and Anderson, B. E.: Asian dust observed  
331 during KORUS-AQ facilitates the uptake and incorporation of soluble pollutants during  
332 transport to South Korea, *Atmos. Environ.*, 224, 117305,  
333 <https://doi.org/10.1016/j.atmosenv.2020.117305>, 2020.

334 Hodzic, A., Bessagnet, B., and Vautard, R.: A model evaluation of coarse-mode nitrate  
335 heterogeneous formation on dust particles, *Atmos. Environ.*, 40, 4158-4171,  
336 <https://doi.org/10.1016/j.atmosenv.2006.02.015>, 2006.

337 Huynh, H. N. and McNeill, V. F.: Heterogeneous Chemistry of  $CaCO_3$  Aerosols with  $HNO_3$  and  
338  $HCl$ , *J. Phys. Chem.*, 124, 3886-3895, <https://doi.org/10.1021/acs.jpca.9b11691>, 2020.

339 Jeong, J. I., Seo, J., and Park, R. J.: Compromised Improvement of Poor Visibility Due to PM  
340 Chemical Composition Changes in South Korea, *Remote Sens.*, 14, 5310,  
341 <https://doi.org/10.3390/rs14215310>, 2022.

342 Kakavas, S. and Pandis, S. N.: Effects of urban dust emissions on fine and coarse PM levels and  
343 composition, *Atmos. Environ.*, 246, 118006,  
344 <https://doi.org/10.1016/j.atmosenv.2020.118006>, 2021.

345 Kutra, I.: Soil Erosion by Wind and Dust Emission in Semi-Arid Soils Due to Agricultural  
346 Activities, *Agronomy*, 10 (1), 89, <https://doi.org/10.3390/agronomy10010089>, 2020.

347 Kim, H., Zhang, Q., and Heo, J.: Influence of intense secondary aerosol formation and long-range  
348 transport on aerosol chemistry and properties in the Seoul Metropolitan Area during spring  
349 time: results from KORUS-AQ, *Atmos. Chem. Phys.*, 18, 7149-7168,  
350 <https://doi.org/10.5194/acp-18-7149-2018>, 2018.

- 351 Kim, H., Zhang, Q., and Sun, Y.: Measurement report: Characterization of severe spring haze  
352 episodes and influences of long-range transport in the Seoul metropolitan area in March  
353 2019, *Atmos. Chem. Phys.*, 20, 11527-11550, <https://doi.org/10.5194/acp-20-11527-2020>,  
354 2020.
- 355 Kim, H., Zhang, Q., Bae, G. N., Kim, J. Y., and Lee, S. B.: Sources and atmospheric processing  
356 of winter aerosols in Seoul, Korea: insights from real-time measurements using a high-  
357 resolution aerosol mass spectrometer, *Atmos. Chem. Phys.*, 17, 2009-2033,  
358 <https://doi.org/10.5194/acp-17-2009-2017>, 2017.
- 359 Lee, H., Honda, Y., Hashizume, M., Guo, Y. L., Wu, C.-F., Kan, H., Jung, K., Lim, Y.-H., Yi, S.,  
360 and Kim, H.: Short-term exposure to fine and coarse particles and mortality: A multicity  
361 time-series study in East Asia, *Environ. Pollut.*, 207, 43-51,  
362 <https://doi.org/10.1016/j.envpol.2015.08.036>, 2015.
- 363 Li, H., Cheng, J., Zhang, Q., Zheng, B., Zhang, Y., Zheng, G., and He, K.: Rapid transition in  
364 winter aerosol composition in Beijing from 2014 to 2017: response to clean air actions,  
365 *Atmos. Chem. Phys.*, 19, 11485-11499, <https://doi.org/10.5194/acp-19-11485-2019>, 2019.
- 366 Li, H., Zhang, Q., Zheng, B., Chen, C., Wu, N., Guo, H., Zhang, Y., Zheng, Y., Li, X., and He,  
367 K.: Nitrate-driven urban haze pollution during summertime over the North China Plain,  
368 *Atmos. Chem. Phys.*, 18, 5293-5306, <https://doi.org/10.5194/acp-18-5293-2018>, 2018.
- 369 Li, T., Bi, X., Dai, Q., Wu, J., Zhang, Y., and Feng, Y.: Optimized approach for developing soil  
370 fugitive dust emission inventory in "2+26" Chinese cities, *Environ. Pollut.*, 285, 117521,  
371 <https://doi.org/10.1016/j.envpol.2021.117521>, 2021a.
- 372 Li, T., Dong, W., Dai, Q., Feng, Y., Bi, X., Zhang, Y., and Wu, J.: Application and validation of  
373 the fugitive dust source emission inventory compilation method in Xiong'an New Area,  
374 China, *Sci. Total Environ.*, 798, 149114, <https://doi.org/10.1016/j.scitotenv.2021.149114>,  
375 2021b.
- 376 Li, T., Ma, S., Liang, W., Li, L., Dai, Q., Bi, X., Wu, J., Zhang, Y., and Feng, Y.: Application of  
377 the high spatiotemporal resolution soil fugitive dust emission inventory compilation method  
378 based on CAMx model, *Atmos. Res.*, 262, 105770,  
379 <https://doi.org/10.1016/j.atmosres.2021.105770>, 2021c.
- 380 Liao, W., Liu, M., Huang, X., Wang, T., Xu, Z., Shang, F., Song, Y., Cai, X., Zhang, H., Kang,  
381 L., and Zhu, T.: Estimation for ammonia emissions at county level in China from 2013 to  
382 2018, *Sci. China Earth Sci.*, 65, 1116-1127, <https://doi.org/10.1007/s11430-021-9897-3>,  
383 2022.
- 384 Liu, H., Jacob, D. J., Bey, I., and Yantosca, R. M.: Constraints from  $^{210}\text{Pb}$  and  $^7\text{Be}$  on wet  
385 deposition and transport in a global three-dimensional chemical tracer model driven by  
386 assimilated meteorological fields, *J. Geophys. Res. Atmos.*, 106, 12109-12128,  
387 <https://doi.org/10.1029/2000JD900839>, 2001.
- 388 Liu, S., Xing, J., Sahu, S. K., Liu, X., Liu, S., Jiang, Y., Zhang, H., Li, S., Ding, D., Chang, X.,  
389 and Wang, S.: Wind-blown dust and its impacts on particulate matter pollution in Northern  
390 China: current and future scenarios, *Environ. Res. Lett.*, 16, 114041,  
391 <http://dx.doi.org/10.1088/1748-9326/ac31ec>, 2021.
- 392 Liu, Y., Gibson, Cain, Wang, H., Grassian, and Laskin, A.: Kinetics of Heterogeneous Reaction  
393 of  $\text{CaCO}_3$  particles with Gaseous  $\text{HNO}_3$  over a Wide Range of Humidity, *J. Phys. Chem. A*,  
394 112, 1561-1571, <https://doi.org/10.1021/jp076169h>, 2008.

- 395 Luo, G., Yu, F., and Schwab, J.: Revised treatment of wet scavenging processes dramatically  
396 improves GEOS-Chem 12.0.0 simulations of nitric acid, nitrate, and ammonium over the  
397 United States, *Geosci. Model Dev.*, 12, 3439-3447 [https://doi.org/10.5194/gmd-12-3439-](https://doi.org/10.5194/gmd-12-3439-2019)  
398 [2019](https://doi.org/10.5194/gmd-12-3439-2019), 2019.
- 399 McNaughton, C. S., Clarke, A. D., Howell, S. G., Pinkerton, M., Anderson, B., Thornhill, L.,  
400 Hudgins, C., Winstead, E., Dibb, J. E., Scheuer, E., and Maring, H.: Results from the DC-8  
401 Inlet Characterization Experiment (DICE): Airborne Versus Surface Sampling of Mineral  
402 Dust and Sea Salt Aerosols, *Aerosol Sci. Tech.*, 41, 136-159,  
403 <https://doi.org/10.1080/02786820601118406>, 2007.
- 404 Mgelwa, A. S., Song, L., Fan, M., Li, Z., Zhang, Y., Chang, Y., Pan, Y., Gurmessa, G. A., Liu, D.,  
405 Huang, S., Qiu, Q., and Fang, Y.: Isotopic imprints of aerosol ammonium over the north  
406 China plain, *Environ. Pollut.*, 315, 120376, <https://doi.org/10.1016/j.envpol.2022.120376>,  
407 2022.
- 408 Noh, H.-j., Lee, S.-k., and Yu, J.-h.: Identifying Effective Fugitive Dust Control Measures for  
409 Construction Projects in Korea, *Sustainability*, 10, 1206,  
410 <https://doi.org/10.3390/su10041206>, 2018.
- 411 Park, S. H., Song, C. B., Kim, M. C., Kwon, S. B., and Lee, K. W.: Study on Size Distribution of  
412 Total Aerosol and Water-Soluble Ions During an Asian Dust Storm Event at Jeju Island,  
413 Korea, *Environ. Monit. Assess.*, 93, 157-183,  
414 <https://doi.org/10.1023/B:EMAS.0000016805.04194.56>, 2004.
- 415 Park, R. J., Oak, Y. J., Emmons, L. K., Kim, C.-H., Pfister, G. G., Carmichael, G. R., Saide, P. E., Cho, S.-  
416 Y., Kim, S., Woo, J.-H., Crawford, J. H., Gaubert, B., Lee, H.-J., Park, S.-Y., Jo, Y.-J., Gao, M., Tang,  
417 B., Stanier, C. O., Shin, S. S., Park, H. Y., Bae, C., and Kim, E.: Multi-model intercomparisons of air  
418 quality simulations for the KORUS-AQ campaign, *Elementa-Sci. Anthropol.*, 9, 00139,  
419 <https://doi.org/10.1525/elementa.2021.00139>, 2021.
- 420 Philip, S., Martin, R. V., Snider, G., Weagle, C. L., van Donkelaar, A., Brauer, M., Henze, D. K.,  
421 Klimont, Z., Venkataraman, C., and Guttikunda, S. K.: Anthropogenic fugitive, combustion  
422 and industrial dust is a significant, underrepresented fine particulate matter source in global  
423 atmospheric models, *Environ. Res. Lett.*, 12, 044018, [https://doi.org/10.1088/1748-](https://doi.org/10.1088/1748-9326/aa65a4)  
424 [9326/aa65a4](https://doi.org/10.1088/1748-9326/aa65a4), 2017.
- 425 Qiu, H., Tian, L. W., Pun, V. C., Ho, K.-f., Wong, T. W., and Yu, I. T. S.: Coarse particulate  
426 matter associated with increased risk of emergency hospital admissions for pneumonia in  
427 Hong Kong, *Respiratory Epidemiology*, 69, 1027, [http://dx.doi.org/10.1136/thoraxjnl-2014-](http://dx.doi.org/10.1136/thoraxjnl-2014-205429)  
428 [205429](http://dx.doi.org/10.1136/thoraxjnl-2014-205429), 2014.
- 429 Shah, V., Jacob, D. J., Moch, J. M., Wang, X., and Zhai, S.: Global modeling of cloud water  
430 acidity, precipitation acidity, and acid inputs to ecosystems, *Atmos. Chem. Phys.*, 20, 12223-  
431 12245, <https://doi.org/10.5194/acp-20-12223-2020>, 2020a.
- 432 Shah, V., Jacob, D. J., Li, K., Silvern, R. F., Zhai, S., Liu, M., Lin, J., and Zhang, Q.: Effect of  
433 changing NO<sub>x</sub> lifetime on the seasonality and long-term trends of satellite-observed  
434 tropospheric NO<sub>2</sub> columns over China, *Atmos. Chem. Phys.*, 20, 1483-1495,  
435 <https://doi.org/10.5194/acp-20-1483-2020>, 2020b.
- 436 Shao, Y. and Dong, C. H.: A review on East Asian dust storm climate, modelling and monitoring,  
437 *Glob. Planet. Change*, 52, 1-22, <https://doi.org/10.1016/j.gloplacha.2006.02.011>, 2006.

438 Stelson, A. W. and Seinfeld, J. H.: Thermodynamic prediction of the water activity,  $\text{NH}_4\text{NO}_3$   
439 dissociation constant, density and refractive index for the  $\text{NH}_4\text{NO}_3$ - $(\text{NH}_4)_2\text{SO}_4$ - $\text{H}_2\text{O}$  system  
440 at 25° C, *Atmos. Environ.*, 16, 2507-2514, [https://doi.org/10.1016/0004-6981\(82\)90142-1](https://doi.org/10.1016/0004-6981(82)90142-1),  
441 1982.

442 Stone, E. A., Yoon, S.-C., and Schauer, J. J.: Chemical Characterization of Fine and Coarse  
443 Particles in Gosan, Korea during Springtime Dust Events, *Aerosol Air Qual. Res.*, 11, 31-43,  
444 <http://dx.doi.org/10.4209/aaqr.2010.08.0069>, 2011.

445 Tang, Y. and Han, G.: Characteristics of major elements and heavy metals in atmospheric dust in  
446 Beijing, China, *J. Geochem. Explor.*, 176, 114-119,  
447 <https://doi.org/10.1016/j.gexplo.2015.12.002>, 2017.

448 Tian, R., Ma, X., Sha, T., Pan, X., and Wang, Z.: Exploring dust heterogeneous chemistry over  
449 China: Insights from field observation and GEOS-Chem simulation, *Sci. Total Environ.*,  
450 798, 149307, <https://doi.org/10.1016/j.scitotenv.2021.149307>, 2021.

451 Travis, K. R., Crawford, J. H., Chen, G., Jordan, C. E., Nault, B. A., Kim, H., Jimenez, J. L.,  
452 Campuzano-Jost, P., Dibb, J. E., Woo, J. H., Kim, Y., Zhai, S., Wang, X., McDuffie, E. E.,  
453 Luo, G., Yu, F., Kim, S., Simpson, I. J., Blake, D. R., Chang, L., and Kim, M. J.: Limitations  
454 in representation of physical processes prevent successful simulation of PM<sub>2.5</sub> during  
455 KORUS-AQ, *Atmos. Chem. Phys.*, 22, 7933-7958, [https://doi.org/10.5194/acp-22-7933-](https://doi.org/10.5194/acp-22-7933-2022)  
456 [2022](https://doi.org/10.5194/acp-22-7933-2022), 2022.

457 Wang, X., Zhang, L., Yao, Z., Ai, S., Qian, Z., Wang, H., BeLue, R., Liu, T., Xiao, J., Li, X.,  
458 Zeng, W., Ma, W., and Lin, H.: Ambient coarse particulate pollution and mortality in three  
459 Chinese cities: Association and attributable mortality burden, *Sci. Total Environ.*, 628-629,  
460 1037-1042, <https://doi.org/10.1016/j.scitotenv.2018.02.100>, 2018a.

461 Wang, Z., Pan, X., Uno, I., Chen, X., Yamamoto, S., Zheng, H., Li, J., and Wang, Z.: Importance  
462 of mineral dust and anthropogenic pollutants mixing during a long-lasting high PM event  
463 over East Asia, *Environ. Pollut.*, 234, 368-378, <https://doi.org/10.1016/j.envpol.2017.11.068>,  
464 2018b.

465 Wang, Z., Pan, X., Uno, I., Li, J., Wang, Z., Chen, X., Fu, P., Yang, T., Kobayashi, H., Shimizu,  
466 A., Sugimoto, N., and Yamamoto, S.: Significant impacts of heterogeneous reactions on the  
467 chemical composition and mixing state of dust particles: A case study during dust events  
468 over northern China, *Atmos. Environ.*, 159, 83-91,  
469 <https://doi.org/10.1016/j.atmosenv.2017.03.044>, 2017.

470 Wesely, M. L.: Parameterization of surface resistances to gaseous dry deposition in regional-scale  
471 numerical models, *Atmos. Environ.*, 23, 1293-1304, [https://doi.org/10.1016/0004-](https://doi.org/10.1016/0004-6981(89)90153-4)  
472 [6981\(89\)90153-4](https://doi.org/10.1016/0004-6981(89)90153-4), 1989.

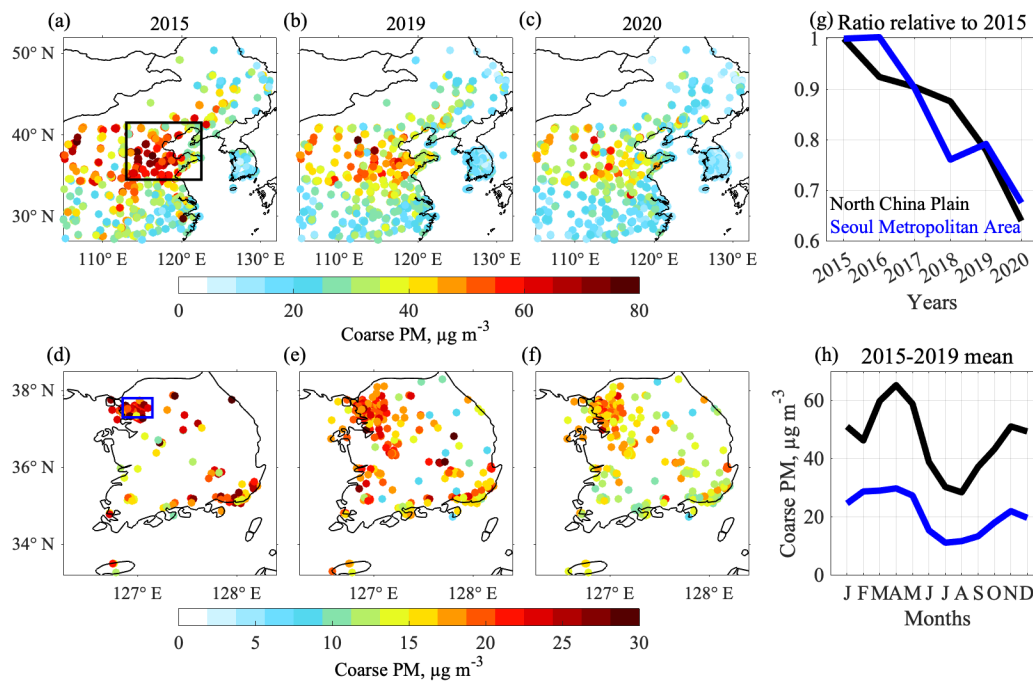
473 Wexler, A. S. and Seinfeld, J. H.: Analysis of aerosol ammonium nitrate: Departures from  
474 equilibrium during SCAQS, *Atmos. Environ. Part A. General Topics*, 26, 579-591,  
475 [https://doi.org/10.1016/0960-1686\(92\)90171-G](https://doi.org/10.1016/0960-1686(92)90171-G), 1992.

476 Woo, J.-H., Kim, Y., Kim, H.-K., Choi, K.-C., Eum, J.-H., Lee, J.-B., Lim, J.-H., Kim, J., and  
477 Seong, M.: Development of the CREATE Inventory in Support of Integrated Climate and  
478 Air Quality Modeling for Asia, *Sustainability*, 12, 7930,  
479 <https://doi.org/10.3390/su12197930>, 2020.

- 480 Wu, Z., Zhang, X., and Wu, M.: Mitigating construction dust pollution: state of the art and the  
481 way forward, *J. Clean. Prod.*, 112, 1658-1666, <https://doi.org/10.1016/j.jclepro.2015.01.015>,  
482 2016.
- 483 Xing, J., Ye, K., Zuo, J., and Jiang, W.: Control Dust Pollution on Construction Sites: What  
484 Governments Do in China?, *Sustainability*, 10, 2945, <https://doi.org/10.3390/su10082945>,  
485 2018.
- 486 Xu, Q., Wang, S., Jiang, J., Bhattarai, N., Li, X., Chang, X., Qiu, X., Zheng, M., Hua, Y., and  
487 Hao, J.: Nitrate dominates the chemical composition of PM<sub>2.5</sub> during haze event in Beijing,  
488 China, *Sci. Total Environ.*, 689, 1293-1303, <https://doi.org/10.1016/j.scitotenv.2019.06.294>,  
489 2019.
- 490 Zhai, S., Jacob, D. J., Wang, X., Liu, Z., Wen, T., Shah, V., Li, K., Moch, J. M., Bates, K. H.,  
491 Song, S., Shen, L., Zhang, Y., Luo, G., Yu, F., Sun, Y., Wang, L., Qi, M., Tao, J., Gui, K.,  
492 Xu, H., Zhang, Q., Zhao, T., Wang, Y., Lee, H. C., Choi, H., and Liao, H.: Control of  
493 particulate nitrate air pollution in China, *Nat. Geosci.*, 14, 389-395,  
494 <https://doi.org/10.1038/s41561-021-00726-z>, 2021a.
- 495 Zhai, S., Jacob, D. J., Brewer, J. F., Li, K., Moch, J. M., Kim, J., Lee, S., Lim, H., Lee, H. C.,  
496 Kuk, S. K., Park, R. J., Jeong, J. I., Wang, X., Liu, P., Luo, G., Yu, F., Meng, J., Martin, R.  
497 V., Travis, K. R., Hair, J. W., Anderson, B. E., Dibb, J. E., Jimenez, J. L., Campuzano-Jost,  
498 P., Nault, B. A., Woo, J. H., Kim, Y., Zhang, Q., and Liao, H.: Relating geostationary  
499 satellite measurements of aerosol optical depth (AOD) over East Asia to fine particulate  
500 matter (PM<sub>2.5</sub>): insights from the KORUS-AQ aircraft campaign and GEOS-Chem model  
501 simulations, *Atmos. Chem. Phys.*, 21, 16775-16791, [https://doi.org/10.5194/acp-21-16775-](https://doi.org/10.5194/acp-21-16775-2021)  
502 [2021](https://doi.org/10.5194/acp-21-16775-2021), 2021b.
- 503 Zhang, Q., Shen, Z., Cao, J., Ho, K., Zhang, R., Bie, Z., Chang, H., and Liu, S.: Chemical profiles  
504 of urban fugitive dust over Xi'an in the south margin of the Loess Plateau, China, *Atmos.*  
505 *Pollut. Res.*, 5, 421-430, <https://doi.org/10.5094/APR.2014.049>, 2014.
- 506 Zhao, G., Chen, Y., Hopke, P. K., Holsen, T. M., and Dhaniyala, S.: Characteristics of traffic-  
507 induced fugitive dust from unpaved roads, *Aerosol Sci. Technol.*, 51, 1324-1331,  
508 <https://doi.org/10.1080/02786826.2017.1347251>, 2017.
- 509 Zheng, B., Zhang, Q., Geng, G., Chen, C., Shi, Q., Cui, M., Lei, Y., and He, K.: Changes in  
510 China's anthropogenic emissions and air quality during the COVID-19 pandemic in 2020,  
511 *Earth Syst. Sci. Data*, 13, 2895-2907, <https://doi.org/10.5194/essd-13-2895-2021>, 2021a.
- 512 Zheng, B., Cheng, J., Geng, G., Wang, X., Li, M., Shi, Q., Qi, J., Lei, Y., Zhang, Q., and He, K.:  
513 Mapping anthropogenic emissions in China at 1 km spatial resolution and its application in  
514 air quality modeling, *Sci. Bull.*, 66, 612-620, <https://doi.org/10.1016/j.scib.2020.12.008>,  
515 2021b.
- 516 Zheng, B., Tong, D., Li, M., Liu, F., Hong, C., Geng, G., Li, H., Li, X., Peng, L., Qi, J., Yan, L.,  
517 Zhang, Y., Zhao, H., Zheng, Y., He, K., and Zhang, Q.: Trends in China's anthropogenic  
518 emissions since 2010 as the consequence of clean air actions, *Atmos. Chem. Phys.*, 18,  
519 14095-14111, <https://doi.org/10.5194/acp-18-14095-2018>, 2018.

520



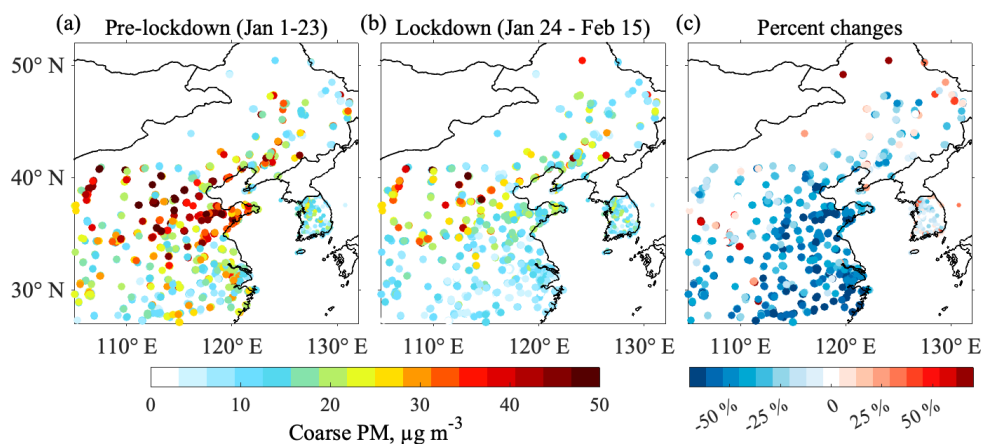


521

522

**Figure 1.** Distributions and trends of coarse PM concentrations over China and South Korea during 2015-2020. Here  
 523 and elsewhere, coarse particulate matter (PM) is defined as particles between 2.5 and 10  $\mu\text{m}$  aerodynamic diameter and  
 524 its concentration is determined by subtracting  $\text{PM}_{2.5}$  from  $\text{PM}_{10}$  in the air quality network data. Panels (a)-(c) show the  
 525 annual mean concentrations in 2015, 2019, and 2020 over China and panels (d)-(f) show the same for South Korea. The  
 526 rectangles in (a) and (d) delineate the North China Plain or NCP (113 - 122.5° E, 34.5 - 41.5° N) and the Seoul  
 527 Metropolitan area or SMA (126.7 - 127.3° E, 37.3 - 37.8° N). Panel (g) shows annual trends relative to 2015 in the  
 528 NCP (197 sites) and the SMA (33 sites) averaged over sites with at least 70% data coverage each year from 2015 to  
 529 2020. Panel (h) shows the mean 2015-2019 seasonality over the NCP and SMA.

530



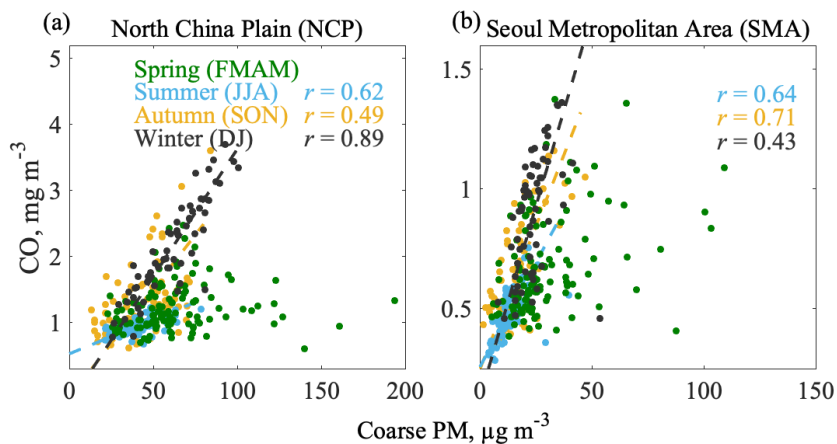
531

532 **Figure 2.** Response of coarse PM to COVID-19 lockdown in China. (a) Coarse PM averaged for the three weeks  
 533 before the China national lockdown (January 1-23, 2020). (b) Coarse PM averaged during the three-week lockdown  
 534 (January 24 - February 15, 2020). (c) Percent changes of coarse PM between lockdown and pre-lockdown periods.

535

536





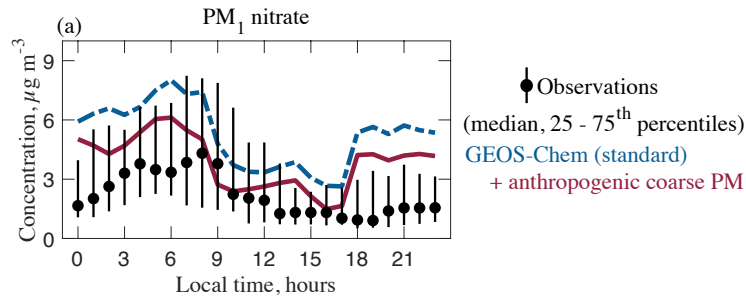
537

538 **Figure 3.** Daily correlations of coarse PM and CO concentrations over the North China Plain (NCP) and Seoul  
 539 Metropolitan Area (SMA) in 2015. Coarse PM and CO concentrations are 24-h averages of air quality network  
 540 observations spatially averaged over the two regions. Also shown are the correlation coefficients and reduced-major-  
 541 axis regression lines except in spring when the correlation is not significant (p-value > 0.05). We include February in  
 542 spring to cover the season of natural dust events (Tang and Han, 2017).

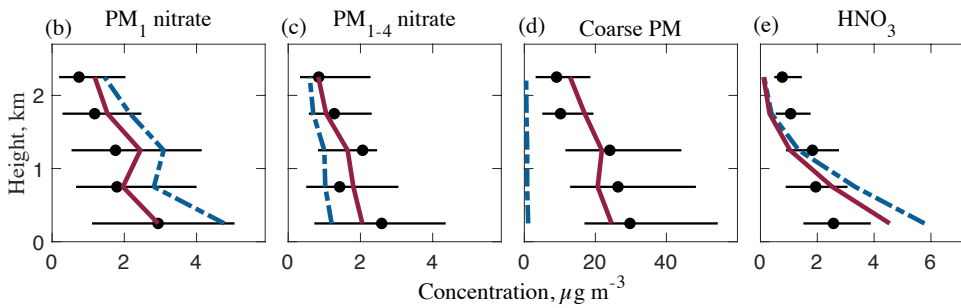
543

544

KORUS-AQ diurnal profile at the KIST surface site in SMA



KORUS-AQ aircraft profiles (< 2.5 km) in SMA



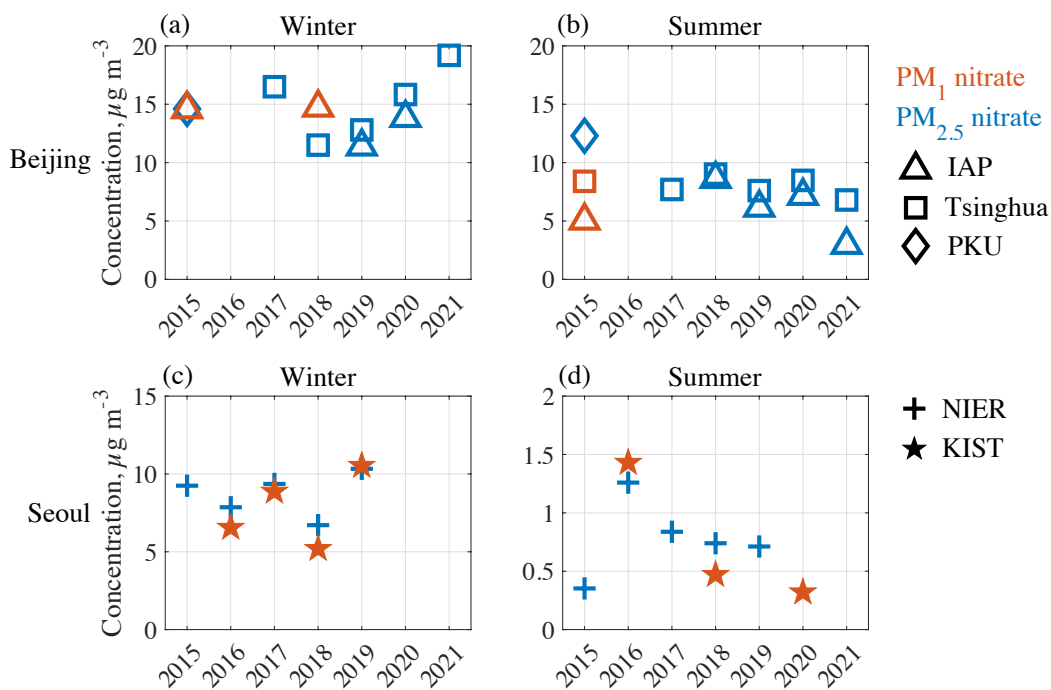
545

546 **Figure 4.** Effect of anthropogenic coarse PM on nitrate concentrations over the Seoul Metropolitan Area (SMA) during  
 547 the KORUS-AQ campaign (May-June 2016). GEOS-Chem model results without (standard) and with anthropogenic  
 548 coarse PM are compared to surface and aircraft observations. (a) Median diurnal variation (error bars are 25<sup>th</sup> and 75<sup>th</sup>  
 549 percentiles) of non-refractory PM<sub>1</sub> nitrate (taken to be ammonium nitrate) at the Korea Institute of Science and  
 550 Technology (KIST) site. (b)-(e) Median vertical profiles of non-refractory PM<sub>1</sub> nitrate, PM<sub>1-4</sub> nitrate, coarse PM (PM<sub>2.5-10</sub>), and HNO<sub>3</sub>  
 551 concentrations for the ensemble of flights over the SMA. Horizontal bars for the observations indicate  
 552 25<sup>th</sup>-75<sup>th</sup> percentiles.

553

554

Observed multi-year fine particulate nitrate in Beijing and Seoul

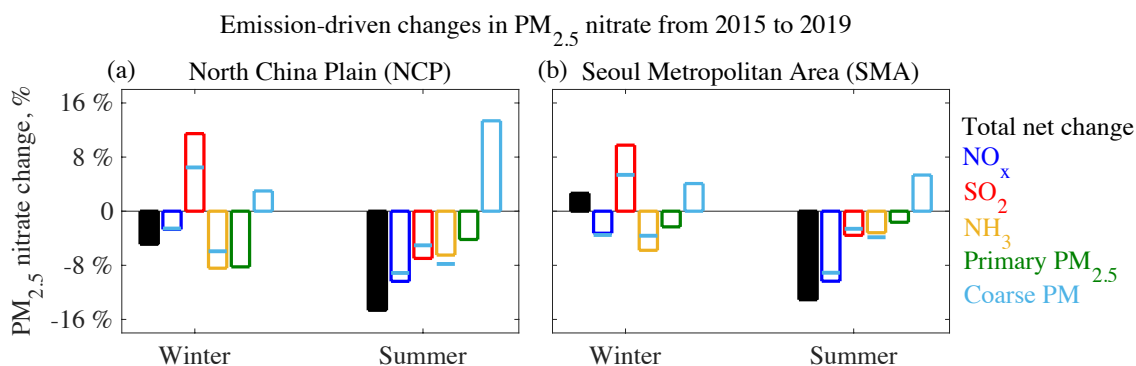


555

556 **Figure 5.** Long-term trend of fine particulate nitrate concentrations in Beijing and Seoul over the 2015-2021 period.  
 557 Mean  $\text{PM}_{1.0}$  or  $\text{PM}_{2.5}$  concentrations in winter and summer are compiled from individual field campaigns in Beijing at  
 558 the Institute of Atmospheric Physics (IAP), Tsinghua University (Tsinghua), and Peking University (PKU) sites and in  
 559 Seoul at the National Institute of Environmental Research (NIER) and Korea Institute of Science and Technology  
 560 (KIST) sites (Table S1). Note the differences in scales between panels.

561

562



563  
564

| Emission changes from 2015 to 2019 |                 |                 |                 |                           |           |
|------------------------------------|-----------------|-----------------|-----------------|---------------------------|-----------|
|                                    | NO <sub>x</sub> | SO <sub>2</sub> | NH <sub>3</sub> | Primary PM <sub>2.5</sub> | Coarse PM |
| NCP                                | -11%            | -54%            | -19%            | -35%                      | -33%      |
| SMA                                | -22%            | -40%            | 0%              | 0%                        | -31%      |

565 **Figure 6.** Emission-driven changes in mean PM<sub>2.5</sub> nitrate from 2015 to 2019 over the NCP and SMA. Results are from  
 566 GEOS-Chem sensitivity simulations including total and individual emission changes over the period, all for the same  
 567 meteorological year (2019) and applied both to China and South Korea (so the effects of NH<sub>3</sub> and primary PM<sub>2.5</sub> over  
 568 the SMA are due to long-range transport from China). Values are seasonal means for winter and summer. The blue  
 569 lines superimposed on the NO<sub>x</sub>, SO<sub>2</sub>, and NH<sub>3</sub> sensitivity bars show the effects from simulations not accounting for the  
 570 effect of HNO<sub>3</sub> uptake by anthropogenic coarse PM.

571